Proceedings of the Twenty-fifth (2015) International Ocean and Polar Engineering Conference **www.isope.org**
Kona, Big Island, Hawaii, USA, June 21-26, 2015

ISBN 978-1-880653-89-0; ISSN 1098-6189

Initial Value Problems for Water Waves in the Presence of a Shear Current

Yan Li, Simen Å. Ellingsen
Department of Energy and Process Engineering, Norwegian University of Science and Technology,
Trondheim, Norway

ABSTRACT

We obtain a general solution for the initial value problems of water waves with a shear current of uniform vorticity beneath the surface in three dimensions. Linearized governing equations and boundary conditions including the effects of gravity, a distributed external pressure disturbance, and constant finite depth, are solved analytically. Results are obtained and corresponding analyses are presented for the special case of an initial pressure impulse condition. Agreement with previous results in the absence of shear current is demonstrated. The results show that a shear current has significant impact on the transient wave motions. The shear current moreover introduced asymmetry between upstream and downstream waves, resulting in asymmetric wave patterns.

KEY WORDS: Initial value problems; shear current; water waves; initial impulsive pressure; free surface elevation

INTRODUCTION

Surface waves in the presence of sub-surface shear currents is both physically fascinating and of great practical importance. Most work on this topic, both analytical and numerical, has been performed in two dimensions, where much progress has been made (e.g., Peregrine, 1976; Teles da Silva & Peregrine, 1988). Of particular interest has been the simplest shear flow model, where vorticity is assumed to be spatially constant. In two dimensions this flow still permits the use of potential theory for linear waves, and the constant vorticity means that complications from critical layers are avoided (Booker & Bretherton, 1967). The literature on this particular flow is extensive; see, e.g. Ellingsen & Brevik (2014) and references therein. In three dimensions, however, progress on the interaction of waves and shear flow is more recent. Ellingsen (2014b) considered ship waves in the presence of shear currents, and also the classical Cauchy-Poisson problem (2014a) with initially prescribed surface shape and velocity.

Classically, two different types of initial value problems have been considered for surface waves. The Cauchy-Poisson variant is one, whereas an alternative is to consider waves generated by applying a localized pressure impulse when the water is initially at rest (Stoker, 2011). When the pressure impulse is short (a Dirac delta function in time), the initial conditions may be reformulated in terms of an initial velocity distribution. A formalism in terms of a general transient external pressure is useful, however, in the study of ship waves, where a "ship" is typically modelled as a travelling pressure source depressing the surface (see Darmon et al. 2014; Ellingsen, 2014b; Raphaël & Gennes 1996). The work presented herein is thus a step towards a more general consideration of non-stationary ship waves.

The presence of a shear current can drastically affect wave motion, resulting in a significantly anisotropic dispersion relation. This results in a widening, narrowing or skewing of ship waves (Ellingsen 2014b), and ring waves from a localized source become elongated and, when shear is strong, cease being ring-shaped at all (Ellingsen 2014a). In the present paper, a general expression is first derived for initial conditions as well as a general, transient external pressure at the free surface. Secondly the related patterns with initial pressure impulse are obtained. For this particular case, a numerical study of patterns and how they are affected by finite depth, vorticity and surface current velocity is presented.

FORMULATION AND SOLUTION OF THE PROBLEM

Description of the Problem

We consider the wave-current system depicted in Figure 1. It is assumed that the water is incompressible, and the water viscosity is negligible. Fluid motion here is rotational due to the shear current, and three dimensional, thus potential theory cannot be used (Ellingsen & Brevik, 2014). We consider water with constant depth *h*.

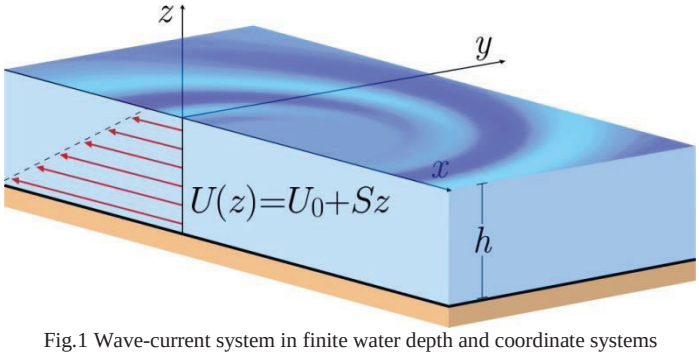

Fig.1 Wave-current system in finite water depth and coordinate systems

Governing equations and linearized boundary conditions

The governing equation for the fluid field is the continuity equation and Euler equation, which may be expressed

$$\nabla \cdot \mathbf{v} = 0 \; ; \tag{1}$$

$$\frac{\mathrm{D}\mathbf{V}}{\mathrm{D}t} = -\frac{1}{\rho}\nabla p - g\boldsymbol{k}, \tag{2}$$

in which operator $\nabla = \frac{\partial}{\partial x}\mathbf{i} + \frac{\partial}{\partial y}\mathbf{j} + \frac{\partial}{\partial z}\mathbf{k}$, $\mathbf{v} = \mathbf{v}(x, y, z, t) = U(z)\mathbf{i} + (u\mathbf{i} + v\mathbf{j} + w\mathbf{k})$, is the fluid velocity, with the basic shear flow $U(z) = Sz + U_0$, and the small velocity perturbations are u, v, w. The density of the fluid is ρ, p is the pressure, and g is the acceleration of gravity.

In this specific problem, boundary conditions include the free surface and sea bottom conditions. For a detailed linearizing process of the boundary conditions, see Ellingsen (2014a). Here, the linearized kinematic and dynamic boundary conditions at the mean free surface are expressed as

$$\left.\begin{aligned} w|_{z=0} &= \left(\frac{\partial \zeta}{\partial t} + U(z)\frac{\partial \zeta}{\partial x}\right)\Big|_{z=0} \\ (p - \rho g\zeta)|_{z=0} &= p_{ext}. \end{aligned}\right\} \quad (3)$$

Where $\zeta = \zeta(x, y, t)$ is the surface elevation compared to the undisturbed surface, and $p_{ext}(x, y, t)$ is the external pressure disturbance, which we assume known. We assume that the external pressure is zero for $t<0$ and has arbitrary time dependence thereafter, but in such a way that its temporal Laplace transform exists. At the sea bottom, the boundary condition is

$$w|_{z=-h} = 0 \quad (4)$$

When viscosity is neglected, the flow is fully determined by Eqs. 1 - 4 and initial conditions.

Fourier Transformation

We introduce Fourier transformations in the xy plane, defined as

$$\left.\begin{aligned} &[u(x, y, z, t), v(x, y, z, t), w(x, y, z, t)] = \\ &\qquad \iint \frac{d^2k}{(2\pi)^2}[\tilde{u}(\boldsymbol{k}, z, t), \tilde{v}(\boldsymbol{k}, z, t), \tilde{w}(\boldsymbol{k}, z, t)]e^{i\boldsymbol{k}\cdot\boldsymbol{r}}, \\ &p(x, y, z, t) - \rho g z = \iint \frac{d^2k}{(2\pi)^2}\tilde{p}(\boldsymbol{k}, z, t)e^{i\boldsymbol{k}\cdot\boldsymbol{r}}, \\ &\zeta(x, y, t) = \iint \frac{d^2k}{(2\pi)^2}\tilde{\zeta}(\boldsymbol{k}, t)e^{i\boldsymbol{k}\cdot\boldsymbol{r}}, \\ &p_{ext}(x, y, t) = \iint \frac{d^2k}{(2\pi)^2}\tilde{p}_{ext}(\boldsymbol{k}, t)e^{i\boldsymbol{k}\cdot\boldsymbol{r}}, \end{aligned}\right\} \quad (5)$$

in which wave vector $\boldsymbol{k} = (k_x, k_y) = (k\cos\theta, k\sin\theta)$, and $\boldsymbol{r} = x\vec{\imath} + y\vec{\jmath}$.

Linearize Eq. 1 and Eq. 2, and apply Fourier transformation to Eq. 1~4, then the continuity and Euler equations could be expressed as:

$$\left.\begin{aligned} &ik_x\tilde{u} + ik_y\tilde{v} + \tilde{w}' = 0, \ \dot{\tilde{u}} + ik_xU\tilde{u} + S\tilde{w} = -ik_x\tilde{p}/\rho, \\ &\dot{\tilde{v}} + ik_xU\tilde{v} = -ik_y\tilde{p}/\rho, \quad \dot{\tilde{w}} + ik_xU\tilde{w} = -\tilde{p}'/\rho \end{aligned}\right\} \quad (6)$$

here, a dot represents derivation with respect to time, a prime with respect to z.

General Solutions in Finite Water Depth

Following the procedure of Ellingsen (2014a) by eliminating $\tilde{u}$, $\tilde{v}$, and $\tilde{p}$, we obtain a Rayleigh equation for $\tilde{w}$ alone,

$$(\partial/\partial t + ik_xU)(\partial^2/\partial z^2 - k^2)\tilde{w} = 0 \quad . \quad (7)$$

The general solution of $\tilde{w}$ has the expression:

$$\tilde{w} = kA(\boldsymbol{k}, t)\sinh k(z + h) + kC(\boldsymbol{k}, t)\cosh k(z + h) + \frac{k^3D(\boldsymbol{k})e^{-ik_xUt}}{k^2 + (k_xSt)^2} \quad (8)$$

in which $A(\boldsymbol{k}, t)$, $C(\boldsymbol{k}, t)$ and $D(\boldsymbol{k})$ are spatially constant. Applying the seabed boundary condition into Eq. 8 yields $C(\boldsymbol{k}, t) = D(\boldsymbol{k}) = 0$. Substituting $\tilde{w}$ back into the equations, we obtain

$$\left.\begin{aligned} &\tilde{w} = kA\sinh k(z + h), \\ &\tilde{p}/\rho = -\left(\dot{A} + ik_xUA\right)\cosh k(z + h) + (iSk_xA/k)\sinh k(z + h) \\ &\qquad + \text{const} \end{aligned}\right\}. \quad (9)$$

Substituting Eq. 9 into the boundary conditions at the free surface yields

$$\left.\begin{aligned} &kA(\boldsymbol{k}, t)\sinh kh = ik_xU_0\tilde{\zeta} + \dot{\tilde{\zeta}} \\ &-\left(\dot{A} + ik_xU_0A\right)\cosh kh + (iSk_xA/k)\sinh kh - g\tilde{\zeta} = \tilde{p}_{ext}/\rho \end{aligned}\right\}, \quad (10)$$

in which U_0 is the current velocity at the still free surface, and we define A_0 as $A(\boldsymbol{k}, 0)$, and $\tilde{\zeta}_0$ as $\tilde{\zeta}(\boldsymbol{k}, 0)$.

We apply a Laplace transform to Eq. 10 and eliminate A to get

$$\bar{\tilde{\zeta}}(\boldsymbol{k}, s) = \overline{f_{I_{ext}}}(\boldsymbol{k}, s)/(s^2 + 2i\omega_1 s + \omega_2^2) \quad , \quad (11)$$

where the Laplace transform is defined as

$$\bar{f}(s) = \int_0^\infty dt\, f(t)e^{-st}, \quad (12)$$

and we have defined the quantities

$$\left.\begin{aligned} &\omega_1 = k_xU_0 - Sk_x\tanh kh\,/(2k), \\ &\omega_2^2 = (k_x^2SU_0/k + gk)\tanh kh - (k_xU_0)^2, \\ &\overline{f_{I_{ext}}}(\boldsymbol{k}, s) = -(k\bar{\tilde{p}}_{ext}(\boldsymbol{k}, s)\tanh kh)/\rho + k\sinh kh\, A_0 \\ &\qquad + [s + ik_xU_0 - (iSk_x/k)\tanh kh]\tilde{\zeta}_0 \end{aligned}\right\}. \quad (13)$$

Hence the free surface elevation could be expressed as

$$\zeta(x, y, t) = \iint \frac{d^2k}{(2\pi)^2}[\tilde{\zeta}(\boldsymbol{k}, t)]e^{i\boldsymbol{k}\cdot\boldsymbol{r}} \quad (14)$$

Where $\tilde{\zeta}(\boldsymbol{k}, t) = \int_\Gamma \frac{ds}{2\pi i}\overline{f_{I_{ext}}}(\boldsymbol{k}, s)e^{st}/(s^2 + 2i\omega_1 s + \omega_2^2)$, and the contour Γ runs from $-i\infty$ to $+i\infty$ to the right of all singularities

After we get the expression of the surface elevation, we can obtain the vertical velocity distributions by eq. 9.

Initial Value Conditions

We shall consider the classical initial condition of an impulsive pressure applied to the surface when the water is initially at rest, which just remains for an infinitesimally short time at $t = 0$, but imparts a finite momentum to the surface. Such a pulse is described by a Dirac delta function. In this paper, we focus on this case within the fully general framework developed above.

Consider a time $t > 0$. The time-dependent pressure disturbance has returned to zero, which means the first term of $\overline{f_{I_{ext}}}(\boldsymbol{k}, s)$ in Eq. 13 is zero. Now performing the inverse Laplace transform gives

$$\begin{aligned} \zeta(x, y, t) = \iint \frac{d^2k}{(2\pi)^2}\{&[kA_0\sinh kh - iSk_x\tilde{\zeta}_0\tanh kh\,/(2k)] \\ &\times \frac{\sin\sqrt{\omega_1^2 + \omega_2^2}t}{\sqrt{\omega_1^2 + \omega_2^2}} + \tilde{\zeta}_0\cos\sqrt{\omega_1^2 + \omega_2^2}t\}e^{i(\boldsymbol{k}\cdot\boldsymbol{r} - \omega_1 t)} \end{aligned} \quad (15)$$

Equation 15 implicates a pressure impulse problem as well as a Cauchy-Poisson problem. In the latter case, $\zeta(x,y,t)$ and $\partial\zeta/\partial t$ are given at t=0, and $p_{ext}(x, y, t) = 0$. With a slight change of formalism, Eq. 13 and Eq. 15 could be expressed as

$$\begin{aligned} \zeta(x, y, t) = \iint \frac{d^2k}{(2\pi)^2}\{&(i\omega_1\tilde{\zeta}_0 + \dot{\tilde{\zeta}}_0)\frac{\sin\sqrt{\omega_1^2 + \omega_2^2}t}{\sqrt{\omega_1^2 + \omega_2^2}} \\ &+ \tilde{\zeta}_0\cos\sqrt{\omega_1^2 + \omega_2^2}t\}e^{i(\boldsymbol{k}\cdot\boldsymbol{r} - \omega_1 t)} \end{aligned} \quad (16)$$

which is identical to Eq. 25 in Ellingsen (2014a) when using the conventions defined therein.

For the second initial case, according to Eq. 16, A_0 and $\tilde{\zeta}_0$ have yet to be determined. A Gaussian distribution is used to define the initial pressure impulse, which we express as

$$p_I(r) = I\delta(t)e^{-(\pi r/a)^2}, \quad (17)$$

wherein a is the width of the pulse, and

$$\left.\begin{aligned} &\tilde{p}_I = I\delta(t)a^2e^{-(ka/2\pi)^2}/\pi \\ &\int_{-\infty}^{+\infty}\delta(t)\,dt = \int_{0^-}^{0^+}\delta(t)dt = 1 \end{aligned}\right\} \quad . \quad (18)$$

Next, we obtain the value of A_0 and $\tilde{\zeta}_0$ by integrating Eq. 10 over t in the interval from 0^- to 0^+, whereby

$$\left.\begin{aligned}\int_{0^-}^{0^+} dt\, kA\sinh kh &= \int_{0^-}^{0^+} dt\, ik_xU_0\tilde{\zeta} + \int_{0^-}^{0^+} dt\,\frac{\partial\tilde{\zeta}}{\partial t}\\ \int_{0^-}^{0^+} dt\,\{-(\dot{A}+ik_xU_0A)\cosh kh + (iSk_xA/k)\sinh kh - g\tilde{\zeta}\} &= \int_{0^-}^{0^+} dt\,\tilde{p}_I/\rho\end{aligned}\right\}. \quad (19)$$

By assumption all perturbation quantities are zero when $t<0$, and we may assume A and ζ to take finite values at $t=0^+$. Hence, from Eq. 19, we obtain

$$\tilde{\zeta}_0 = 0, \quad A_0 = -\frac{a^2Ie^{-(ka/2\pi)^2}}{\pi\rho\cosh kh}. \quad (20)$$

Therefore, the surface elevation could be expressed as

$$\zeta(x,y,t) = \iint \frac{d^2k}{(2\pi)^2}\{-\frac{ka^2Ie^{-(ka/2\pi)^2}\tanh kh}{\rho\pi}\frac{\sin\sqrt{\omega_1^2+\omega_2^2}t}{\sqrt{\omega_1^2+\omega_2^2}}e^{i(\boldsymbol{k}\cdot\boldsymbol{r}-\omega_1t)}\}. \quad (21)$$

In order to better evaluate effects of velocity, vorticity and water depth, we introduce the non-dimensional quantities using similar rescaling rules as that of Ellingsen (2014a) , defined in table. 1. Fr_{U_0} and Fr_s are "surface current Froude number" and "shear Froude number", respectively, based on the current velocity at the surface U_0 and velocity *bS*. In terms of non-dimensional quantities, the surface elevation could be expressed as

$$\frac{\zeta}{a} = \int_0^{2\pi} d\gamma \int_0^{\infty} \frac{-K^2PIe^{-\left(\frac{K}{2\pi}\right)^2}\tanh KH\sin T\sqrt{(Fr_s\cos\gamma\tanh KH)^2+K\tanh KH}}{4\rho\pi^3\sqrt{(Fr_s\cos\gamma\tanh KH)^2+K\tanh KH}} e^{i(\boldsymbol{K}\cdot\boldsymbol{R}-(KFr_{U_0}\cos\gamma-Fr_s\cos\gamma\tanh KH)T)}dK \quad . \quad (22)$$

Table 1. Physical V.S. dimensionless quantities

Physical quantities	Non-dimensional quantities
ζ	ζ/a
h	$H=h/a$
r ($\boldsymbol{r}$)	$R=r/a$ ($\boldsymbol{R}=\boldsymbol{r}/a$)
(x,y)	$(X,Y)=(x/a,y/a)$
t	$T=t/\sqrt{a/g}$
$\omega_{1,2}$	$\Omega_{1,2}=\omega_{1,2}\sqrt{a/g}$
k ($\boldsymbol{k}$)	$K=ak$ ($\boldsymbol{K}=a\boldsymbol{k}$)
U_0	$Fr_{U_0}=U_0/\sqrt{ag}$
S	$Fr_s=S\sqrt{a/g}$
I	PI$=I/(\rho a\sqrt{ag})$

LIMITING CASES AND NUMERICAL EXAMPLES

Dispersion Relation

From eq. 10-13, we can obtain the dispersion relation which could be expressed as

$$\left[\omega-k_xU_0+\frac{Sk_x\tanh kh}{2k}\right]^2 = gk\tanh kh + (Sk_x\tanh kh)^2/(4k^2) \quad (23)$$

in which ω is the absolute frequency. This relation reduces to the well known case (e.g., Mei (1979)) when the current is uniform (i.e. S=0). When there is no current at all, eq. 23 is obviously the classical dispersion relation $\omega^2=gk\tanh kh$.

The intrinsic frequency σ could be defined in the expression as

$$\sigma = \omega - k_xU_0 = \pm\sqrt{gk\tanh kh+\left(\frac{Sk_x\tanh kh}{2k}\right)^2}-\frac{Sk_x\tanh kh}{2k} \quad (24)$$

In this perspective, we can define the group velocity relative to the surface velocity

$$\boldsymbol{C}_g = \nabla_{\boldsymbol{k}}\sigma = \frac{\partial\sigma}{\partial k_x}\mathbf{i}+\frac{\partial\sigma}{\partial k_y}\mathbf{j} = \frac{\partial\sigma}{\partial k}\mathbf{e}_k + \frac{1}{k}\frac{\partial\sigma}{\partial\theta}\mathbf{e}_\theta, \quad (25)$$

where $\mathbf{e}_k$ and $\mathbf{e}_\theta$ are unit vectors in polar coordinate Fourier space.

Vertical Velocity Distributions

From eq. 20 we see that the initial pressure impulse at time $t=0^+$ directly results in an initial surface velocity distribution given by A_0, subsequently developing into an outward propagating surface wave.

Fig.1 depicts the vertical velocity distributions for given initial pressure impulse. It may be seen in Fig. 1 that, at $t=0^+$, the main vertical velocity disturbance caused is focused in the region $r\le a$. Outside this region, the vertical velocity is relatively small. It is obvious that the initial velocity will predominately have the opposite sign to the initial pressure impulse.

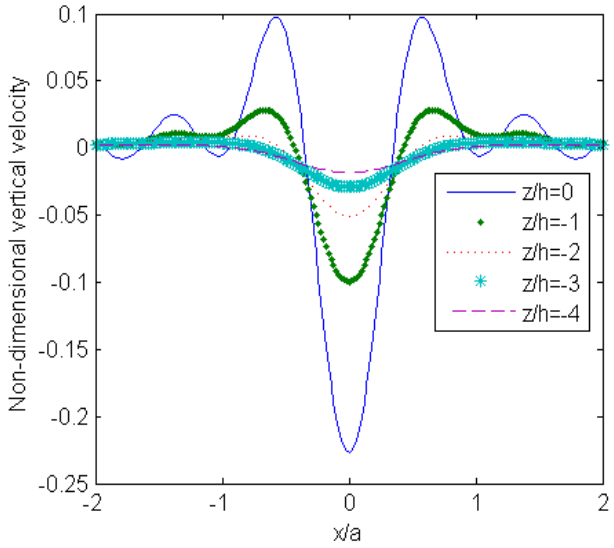

Figure 1. Non-dimensional vertical velocity distributions $W=w/\sqrt{ga}$ at *t=0* as *H=20*, *PI*= 2e-4.

The Effect of Water Depth

Solutions in infinite water depth

By taking the deep water limit of solutions in finite water depth, we can obtain the specific solutions for infinite water depth, which can be expressed as

$$\left.\begin{aligned}\tilde{w} &= kAe^{kz}\\ \tilde{p}/\rho &= -[\dot{A}+ik_xA(U+S/k)]e^{kz}+\text{Const}\\ \tilde{\zeta}(\boldsymbol{k},t) &= \int_\Gamma \frac{ds}{2\pi i}\frac{-k\tilde{\bar{p}}_{ext}(\boldsymbol{k},s)/\rho+kA(\boldsymbol{k},0)+[s+ik_x(U_0-S/k)]\tilde{\zeta}(\boldsymbol{k},0)}{(s^2+2i\omega_1s+\omega_2^2)}e^{st}\end{aligned}\right\} \quad (26)$$

Here, $\omega_1=k_xU_0-Sk_x/(2k)$, and $\omega_2^2=gk+k_x^2SU_0/k-(k_xU_0)^2$.

For the corresponding Cauchy-Poisson initial value problem, we obtain the same expression of surface elevation as given in eq. 16, with ω_1 and ω_2 defined as in eq. 26.

For the second initial value problem, we can get the solution of surface elevation expressed as

$$\frac{\zeta(X,Y,T)}{a} = -\text{PI}\iint\frac{d^2K}{(2\pi)^2}K\frac{\sin\sqrt{\Omega_1^2+\Omega_2^2}T}{\sqrt{\Omega_1^2+\Omega_2^2}}e^{i(\boldsymbol{K}\cdot\boldsymbol{R}-\Omega_1T)-(K/2\pi)^2} \quad (27)$$

In which Ω_1 and $\Omega_1$are defined as before. The exponential ensures that the main contribution comes from $K \lesssim 2\pi$.

Eq. 27 corresponds to Stoker (2011, p.159) when no current is included and assuming the same initial pressure distribution.

The dispersion relation in infinite water depth could be expressed as

$$\sigma = \omega - k_x U_0 = \pm\sqrt{gk + \left(\frac{S}{2}\cos\theta\right)^2} - \frac{S}{2}\cos\theta. \quad (28)$$

According the eq. 25, we can get the relative group velocity along the direction of phase propagation expressed as

$$C_g = \frac{1}{2}\sqrt{\frac{g}{k}}\frac{1}{\sqrt{1+(S\cos\theta)^2/(4k)}} < \frac{1}{2}\sqrt{\frac{g}{k}}. \quad (29)$$

And the relative phase velocity c could be expressed as

$$c = \sigma/k = \sqrt{\frac{g}{k}}\sqrt{1+\frac{1}{4gk}S^2\cos^2\theta} - \frac{S}{2k}\cos\theta \lesseqgtr \sqrt{\frac{g}{k}} \quad (30)$$

As discussed by Ellingsen (2014a) we may disregard the $\pm$ in Eq. 28 when considering the wave velocities, since these correspond to (positive) velocities in opposite directions, and there is a unique positive phase and group velocity in each direction θ. Eqs. 29 and 30 reveal that the relative phase velocity is greater than the group velocity in every wave propagating direction, as one expects for gravity waves. Note moreover how the presence of the shear flow can increase or decrease the phase velocity, but only decrease the group velocity.

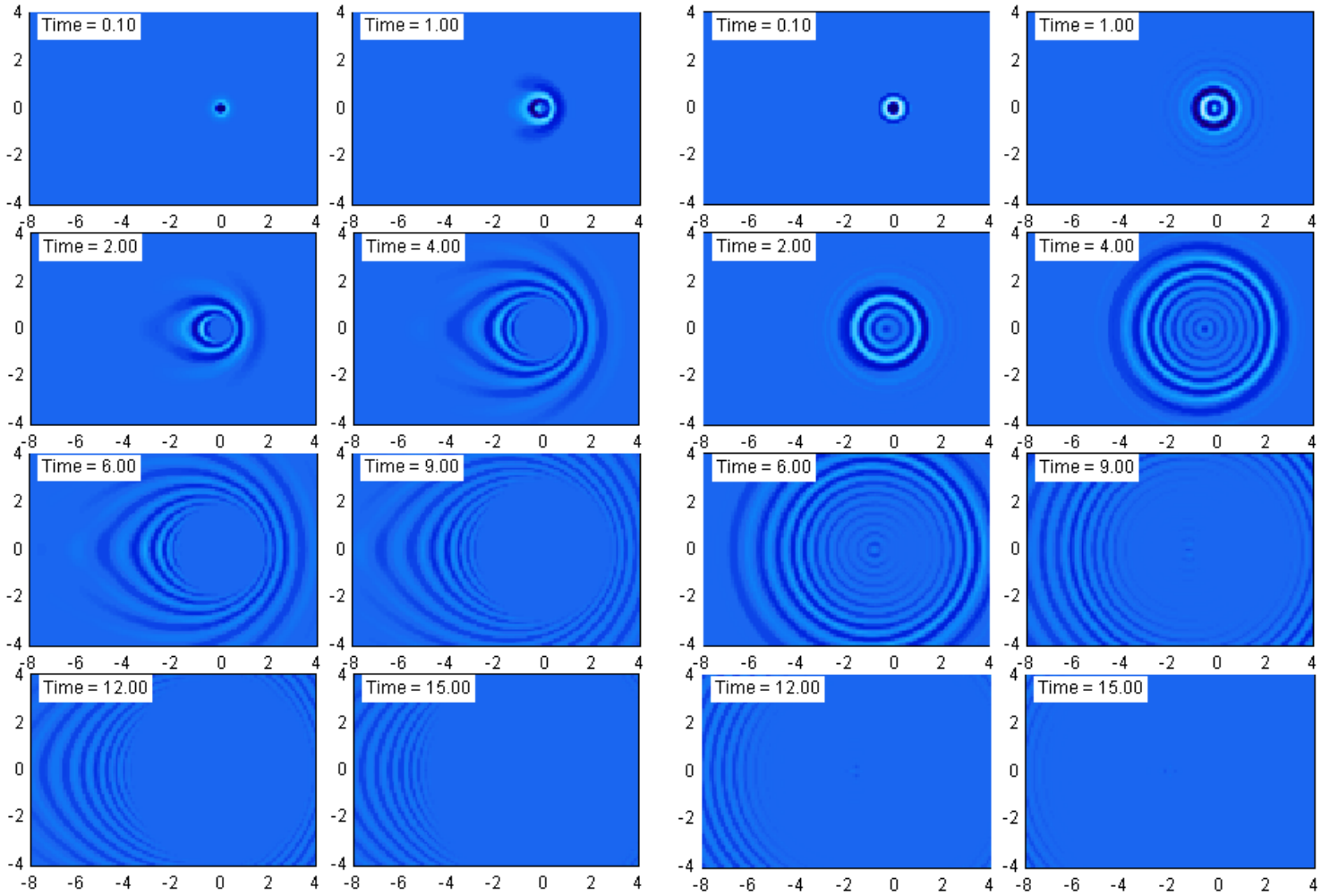

(a) Deep waters (b) Shallow waters

Figure 2. Waves of deep and shallow waters at different times T. In all panels Fr_s=1, Fr_{U_0}=0, and PI=2e-4. Left 8 panels : H=20, right 8 panels: H=0.05. Areas in this and all below figures where $\zeta > 0.2\,\zeta_{\max}(X,Y,T=0.1)$ are white, $\zeta < -0.2\zeta_{\max}(X,Y,T=0.1)$ are black, with linear colour gradient for amplitudes in between.

Limit of shallow water

We consider the shallow water situation, when $h \ll 1$. Then, $\tanh kh \sim kh$. From Eq. 23~Eq. 25 we obtain

$$C_g \approx c \approx \sqrt{gh + \left(\frac{Sh}{2}\cos\theta\right)^2} - \frac{Sh}{2}\cos\theta\,. \quad (31)$$

Eq. 31 shows that the relative phase and group velocities coincide when the water depth is small compared to a wavelength, and there is no dispersion despite the sub-surface shear current. However, velocity varies with the direction of wave propagation due to the existence of shear current. The lack of dispersion means that wave patterns retain their ring shape as they propagate.

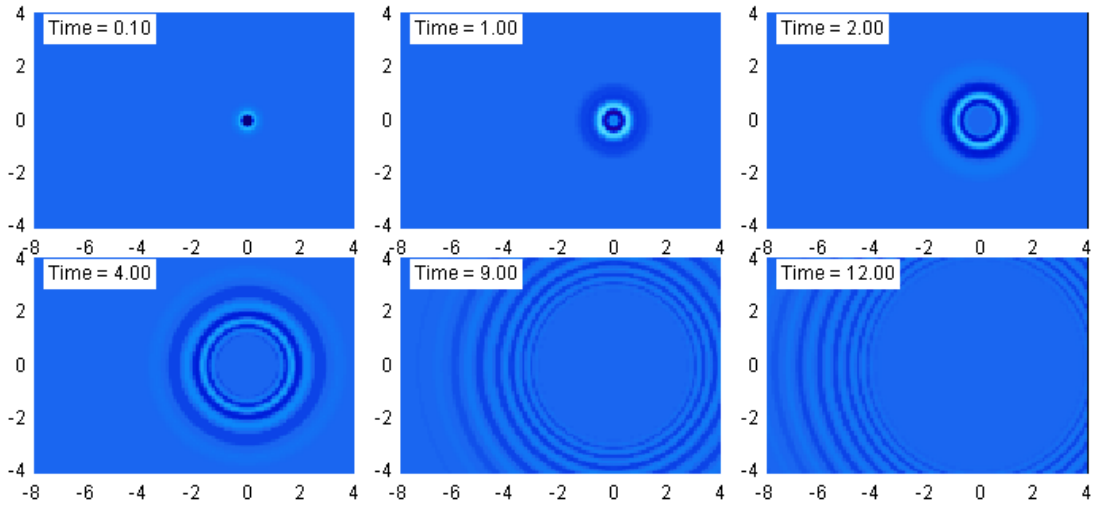

(a) Zero shear current, Fr_s=0

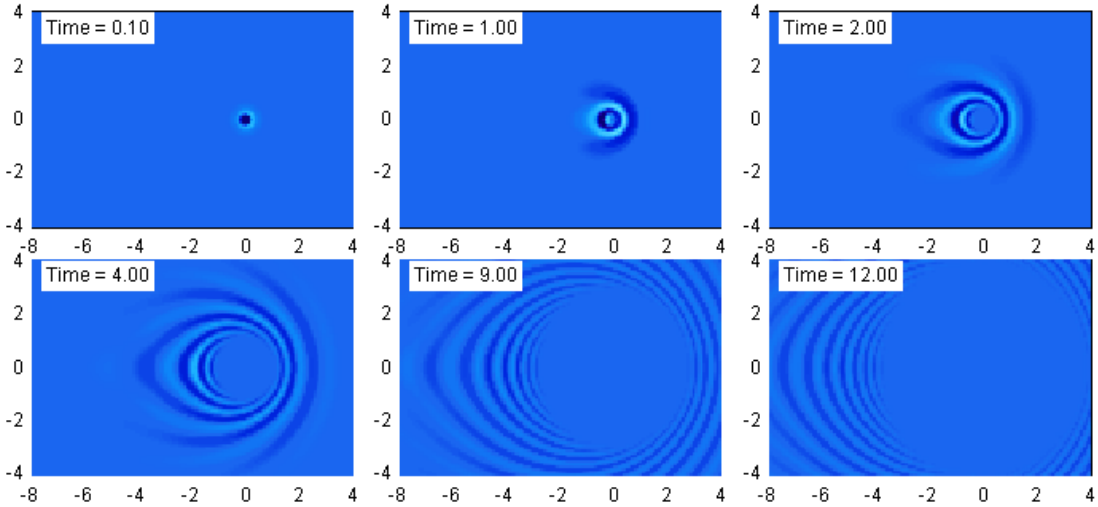

(b) Moderate shear current, Fr_s=1

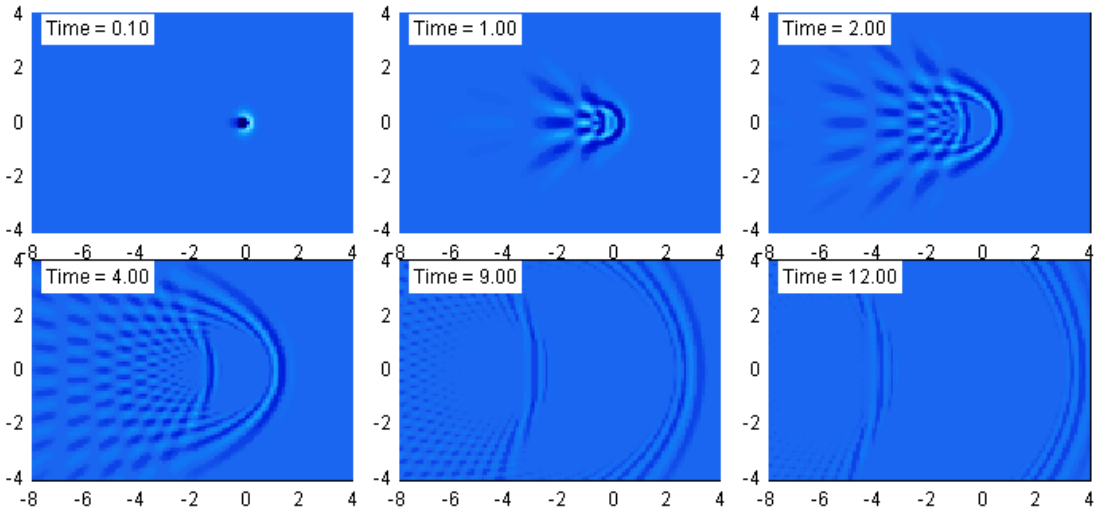

(c) Strong shear current, Fr_s=5

Figure 3. Waves with different shear Froude numbers at different times T. In all panels: Fr_{U_0}=0, PI=2e-4 and H=20. Colour scaling is as in figure 2.

Fig. 2 shows wave patterns at deep (H=20) and shallow (H=0.05) waters at different times with moderate shear current. In the figure, a moderate shear Fr_s=1 is considered and the surface current velocity (Fr_{U_0}=0) is ignored. It is obvious from Fig.2 that the shear current has different influence upon waves in deep and shallow water. Effects of the shear current are more prominent in deep waters. This accords to eq. 29, 30 and eq. 31. The effects of shear in shallow waters are diminished, and the lack of dispersion is apparent from the stability of the ring shapes as they propagate. These observations concur with those of Ellingsen (2014a).

The previous section has shown that the vorticity has different degree of influence in deep and shallow waters. Consider now strong, moderate and zero shear in deep waters, without the surface current velocity in order to simplify the problem. The situation is shown in Fig. 3. In Fig. 3, we can observe that a clear asymmetry is created by the shear current upon the waves from the symmetrical initial pressure disturbance. When the shear is strong enough, the waves fronts are no longer ring shaped, as can be seen in Fig. 3-c.

THE DISPERSION RELATION AND ITS SOLUTIONS

In the following we discuss the dispersion relation further. According to eq. 23, 25, 28~31, it is obvious that the surface current velocity contributes only to the *absolute* phase/group velocity. Consider now a plane wave of a certain frequency ω propagating in a given direction θ, having dispersion relation

$$\omega = \text{const} = kU_0\cos\theta - \frac{S\cos\theta}{2} \pm \sqrt{gk + \frac{(S\cos\theta)^2}{4}}. \qquad (32)$$

Generally, a propagating plane wave has the form $e^{i(\boldsymbol{k}\cdot\boldsymbol{r}-\omega t)}$. When we introduce a Galilean transformation $\boldsymbol{r}' = \boldsymbol{r} - \boldsymbol{U_0}t$, a progressive wave in the rest frame may be written as

$$e^{i(\boldsymbol{k}\cdot\boldsymbol{r}-\omega t)} = e^{i[\boldsymbol{k}\cdot(\boldsymbol{r}'+\boldsymbol{U_0}t)-\omega t]} = e^{i[\boldsymbol{k}\cdot\boldsymbol{r}'-(\omega-\boldsymbol{k}\cdot\boldsymbol{U_0})t]}\ . \qquad (33)$$

Thus in the moving frame the effective frequency is

$$\omega_e = \omega - kU_0\cos\theta \qquad (34)$$

in which θ denotes the angle between wave number vector $\boldsymbol{k}$ and the x axis. The result of eq. 34 is the well-known Doppler effect whereby the frequency of a wave depends upon the frame of reference: $\omega_e \lessgtr \omega$ if $U_0\cos\theta \gtrless 0$.

The dispersion relation eq. 32 could be solved graphically from the intersection of the straight line $y = \omega - kU_0\cos\theta$ and the curves $y = \pm\sigma(k)$ with $\sigma(k)$ from Eq. 28. This is shown in Fig. 4. Fig. 4 is quite similar to figure of Mei (1979, p99) when S=0.

The number of solutions to the dispersion relation depends on the sign of U_0. For $\cos\theta > 0$ (waves propagating towards the right, i.e., positive values of x) , and $U_0 > 0$ there are two possible waves of frequency ω whose wavelengths are shorter and longer than that of zero surface velocity, respectively, and of which the slower one (short wavelength) travels more slowly than the water surface in the absolute system. When $U_0 < 0$ there can be 0, 1 or 2 solutions, depending on the magnitude of $U_0\cos\theta$.

For $\cos\theta < 0$ (waves propagating towards the left), we must distinguish between two different situations, namely whether ω is greater or smaller than $S|\cos\theta|$. When there is no surface current, $S|\cos\theta|$ is the smallest possible wave frequency, whereas introduction of a surface current allows waves of arbitrarily small frequency to fulfil the dispersion relation, as shown in figure 4c.

Whenever $\omega > S|\cos\theta|$, the situation for left-propagating waves resembles that for right-directed propagation. A single solution exists when $U_0 = 0$, and when $U_0 < 0$, two wave numbers satisfy the dispersion relation, one of whose wavelengths is shorter than it would be in absence of surface velocity, the other longer. When $U_0 > 0$ there can be 0, 1 or 2 solutions, depending on the magnitude of $U_0\cos\theta$.

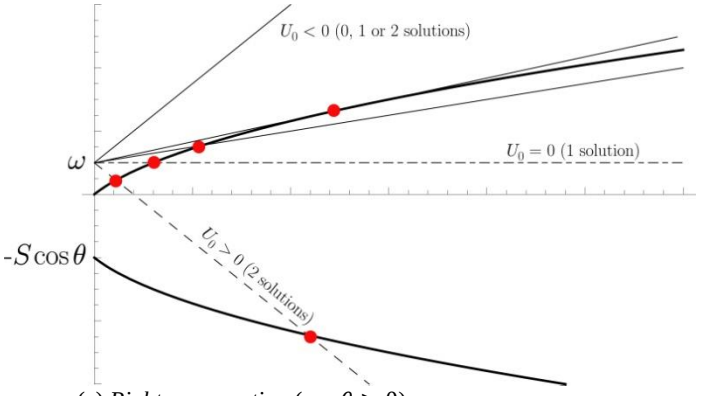

(a) *Right-propagating* ($\cos\theta > 0$)

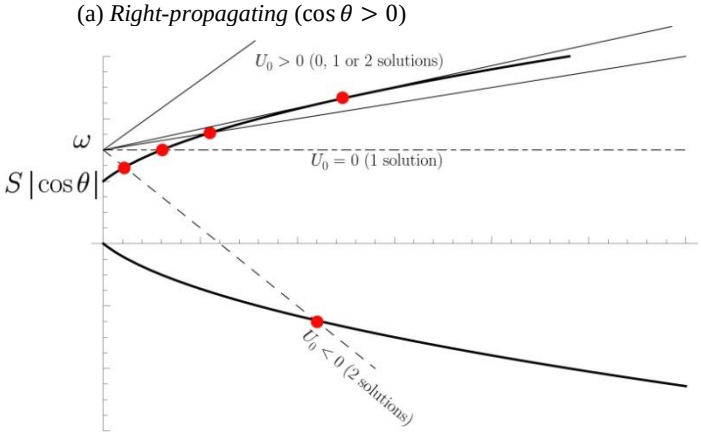

(b) *Left-propagating* ($\cos\theta < 0$), $\omega > S|\cos\theta|$

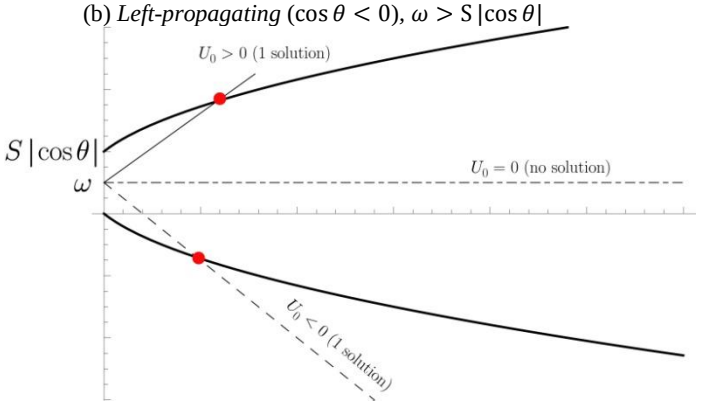

(C) *Left- propagating* ($\cos\theta < 0$), $\omega < S|\cos\theta|$

Figure 4. Graphical solution of Eq. 34.

CONCLUSIONS

In this paper we obtained a general solution of the problem of surface waves in the presence of shear current beneath the water surface, including both initial conditions and time-dependent external pressure. Solutions are obtained in both finite and infinite water depth. As a special case, corresponding analyses are carried out with a distributed external impulsive pressure at t=0.

By numerical simulations we showed how the impulsive pressure, which gives rise to an initial velocity distribution in the fluid, creates a "ring wave" surface elevation pattern at subsequent times.

An obvious effect of shear current of uniform vorticity is to create asymmetry of the wave motion between upstream and downstream directions. Moreover, we confirmed a previous observation that vorticity of the current has more prominent influence in deep waters.

By analyzing the dispersion relation for a steady phase of given frequency in deep waters, we showed that different combinations of the shear vorticity and surface current velocity will result in dramatic discrepancies in wave motions. We categorized three different situations depending on whether waves are travelling towards the right (positive x) or left (negative x), and in the latter case, on the relative values of ω and $S|\cos\theta|$, θ being the angle between wave vector and x axis.

REFEREMCES

Booker, J. R. & Bretherton, F. P. (1967), "The critical layer for internal gravity waves in a shear flow" *Journal of Fluid Mechanics*, vol. 27, pp. 513-539.

Darmon, A., Benzaquen, M, & E. Raphaël (2014), "Kelvin wake pattern at large Froude numbers", *Journal of Fluid Mechanics*, vol. 738, R3.

Ellingsen, S. Å. & Brevik, I. (2014), "How linear surface waves are affected by a current with constant vorticity", *European Journal of Physics*, vol. 35, 025005.

Ellingsen, S. Å. (2014a), "Initial Surface disturbance on a shear current: the Cauchy-Poisson problem with a twist", *Physics of Fluids*, vol. 26, 082104.

Ellingsen, S. Å. (2014b), "Ship waves in the presence of uniform vorticity", *Journal of Fluid Mechanics*, vol. 72, R2.

Mei, C. C. (1979). *The applied dynamics of ocean surface waves*, 1989.Singapore, World Scientific.

Peregrine, D. H. (1976) "Interaction of water waves and currents" *Advances in Applied Mechanics*, vol 16, pp. 9-117.

Raphaël, E & Gennes, D. (1996), "Capillary gravity waves caused by a moving disturbance-wave resistance", *Physical Review*, vol.53, no.4, pp. 3448-3455.

Stoker, James Johnston (2011), *Water waves: The mathematical theory with applications*. Vol. 36. John Wiley & Sons.

Teles da Silva, A. F. & Peregrine, D. H. (1988), "Steep, steady surface waves on water of finite depth with constant vorticity", *Journal of Fluid Mechanics*, vol. 195, pp. 281-302.